AJNR

Preliminary experience with selective laser sintering models of the human temporal bone.

R A Levy, S Guduri and R H Crawford

This information is current as of August 13, 2025.

Preliminary Experience with Selective Laser Sintering Models of the Human Temporal Bone

Richard A. Levy, Sashidhar Guduri, and Richard H. Crawford

PURPOSE: To assess the accuracy of three-dimensional models of the human temporal bone generated from CT data. **METHODS:** Thin-section CT of a left human cadaveric temporal bone was performed using multiple-scan planes (axial, coronal, and sagittal) at 1.5-mm section thickness and 0.25-mm pixel size with an edge-enhancement two-dimensional algorithm. CT data were converted to toggle point format based upon a threshold value of 200 (approximately −830 HU) obtained from prior experimentation with a CT phantom. Selective laser sintering of polycarbonate powder was performed at a beam diameter of 0.060 inches (1.5 mm), 100 scan lines per inch, layer thickness of 0.010 inches (0.25 mm), and layer repeat factor of 4. The polycarbonate models were then scanned in the axial, coronal, and sagittal planes and compared with the original CT data. Anatomic dissection of the models was performed for further verification of the imaging findings. **RESULTS:** Models of high anatomic accuracy were generated. Shortening by a factor of 0.67 along the Z axis secondary to the layer repeat factor of 4 resulted in distortion of the models. Distortion in the XY plane ranged from 0% to 20%. Differences in model accuracy based on the initial CT scan plane were observed. A significant amount of nonsintered or partially sintered polycarbonate resulted in intermediate density on the CT images. **CONCLUSIONS:** Selective laser sintering can result in accurate modeling of detailed anatomic structures in the human temporal bone. Further investigation of materials and factors contributing to the accuracy of selective laser sintering in the manufacturing of high-resolution anatomic models is warranted.

Index terms: Temporal bone, anatomy; Temporal bone, computed tomography; Models, anatomic; Computed tomography, technique; Computed tomography, experimental

Computer-generated anatomic modeling using radiologic data is a well-known entity. Various technologies have been used in the development of anatomic models and prostheses. These technologies include multiaxis milling, stereo lithography, and selective laser sintering (1). Our purpose in this research is to demonstrate the accuracy of selective laser sintered models of the human temporal bone. A qualitative comparison with other anatomic modeling technologies will be discussed.

Methods

Thin-section computed tomography (CT) of a left human cadaveric temporal bone was performed using multiple scan planes (axial, coronal, and sagittal) at a 1.5-mm section thickness and 0.25-mm pixel size with an edge-enhancement two-dimensional algorithm on a General Electric (Milwaukee, Wis) 9800 CT scanner. CT data were networked from the Department of Radiology at the University of Michigan to the Department of Mechanical Engineering at the University of Texas at Austin via an Internet file transfer protocol file. CT data were converted to toggle point format (linear scalar transformation) resulting in a threshold value of 200 (approximately −830 HU) obtained from prior experimentation with a CT phantom. Selective laser sintering of polycarbonate powder was performed with a 25 W carbon dioxide laser with power centered at 14 W at a beam diameter of 0.060 inches (1.5 mm), 100 scan lines per inch, polycarbonate layer thickness of 0.010 inches (0.25 mm), and layer repeat factor of 4. The polycarbonate models were then rescanned, respectively, in the axial, coronal, and sagittal planes and compared with the
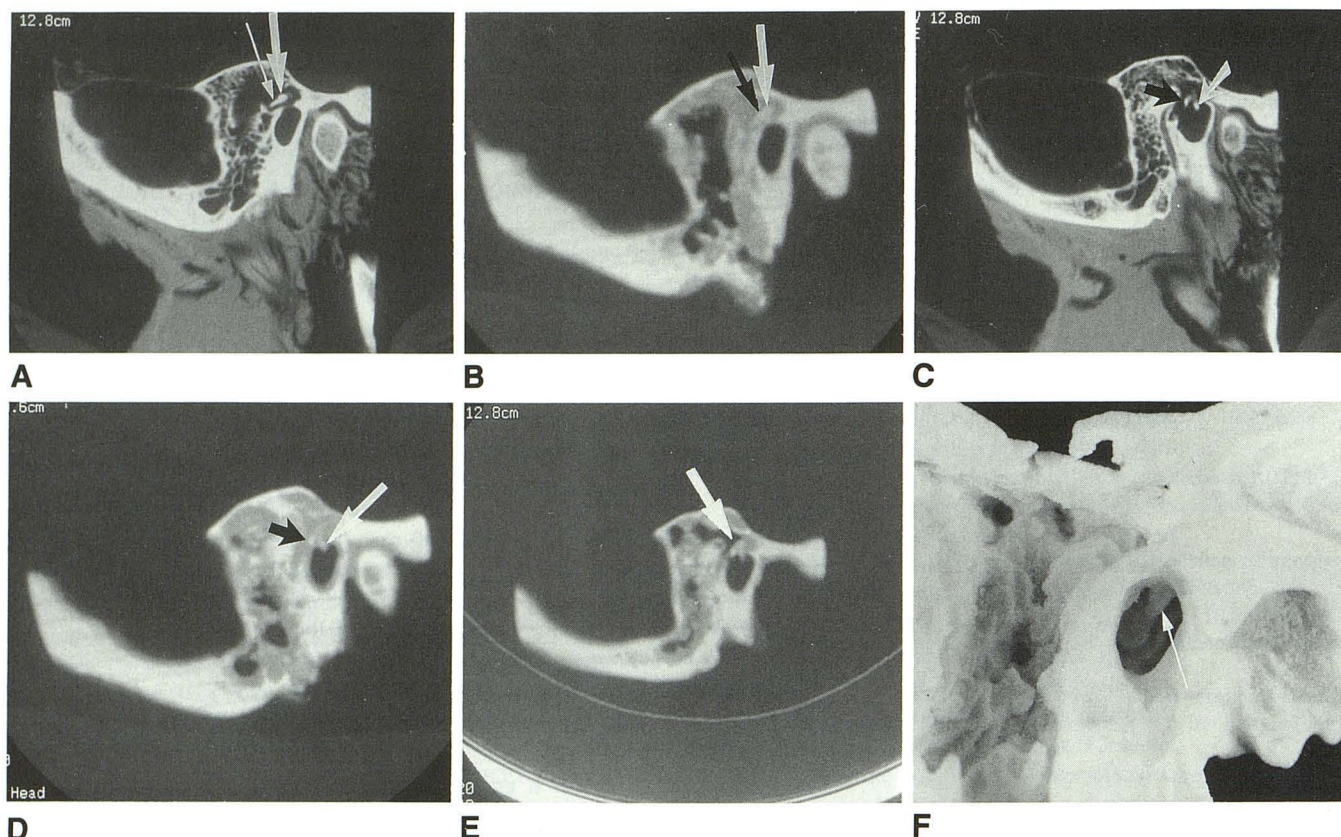
Fig. 1. *A*, Sagittal CT image of a left human cadaveric temporal bone. The *thick arrow* indicates the head of malleus. The *thin arrow* indicates the body of incus.

B, Sagittal CT image of polycarbonate laser-sintered model generated from sagittal CT data and corresponding to CT image in A. The *white arrow* indicates the head of malleus. *Black arrow* indicates the body of incus. Ossicles appear less distinct than on CT imaging.

C, Sagittal CT image medial to plane in A and B. The white arrow indicates the manubrium of malleus. *Black arrow* indicates the long process of incus.

D, Sagittal CT image of polycarbonate temporal bone model through imaging plane in C. The *white arrow* indicates the manubrium of malleus. The *black arrow* indicates the long process of incus.

E, Sagittal CT image of polycarbonate temporal bone model as in D after simulated mastoidectomy. The *white arrow* indicates the resected area of loose polycarbonate powder in middle ear cavity, now with normal air density. Ossicles are better modeled than in Figures 2 and 3.

F, Postdissection polycarbonate model of the human cadaveric temporal bone specimen in A to E. Mirror-image modeling occurs by selecting the last CT section as the starting point for toggle point conversion before laser sintering. The *white arrow* indicates the manubrium of malleus.

original CT data. Anatomic dissection of the models was performed for further verification of the imaging findings.

Results

Models of high anatomic accuracy were generated as verified by measurement of the margins of the models. Measurements from images of scanned models were compared with similar measurements from original CT data (Figs 1, 2, and 3). Shortening along the Z axis (defined as the craniocaudal axis for axial data, the anteroposterior axis for coronal data, and the mediolateral axis for sagittal data) averaged 0.67 of the original specimen length along the Z axis, consistent with use of a layer repeat factor of 4 instead of 6. (A layer repeat factor of 6, at 0.010-inch [0.25-mm] thick polycarbonate layers, would have resulted in no distortion along the Z axis, equaling the initial 1.5-mm CT section thickness.)

No distortion in the XY plane (defined as the image orientation on the 2-D CT video display) was observed for models generated from axial or sagittal data. A 10% reduction in transverse dimension and a 20% reduction in height were observed with the model generated from coronal data. Differences in model accuracy based on initial CT scan plane were observed (Figs 1–3). A
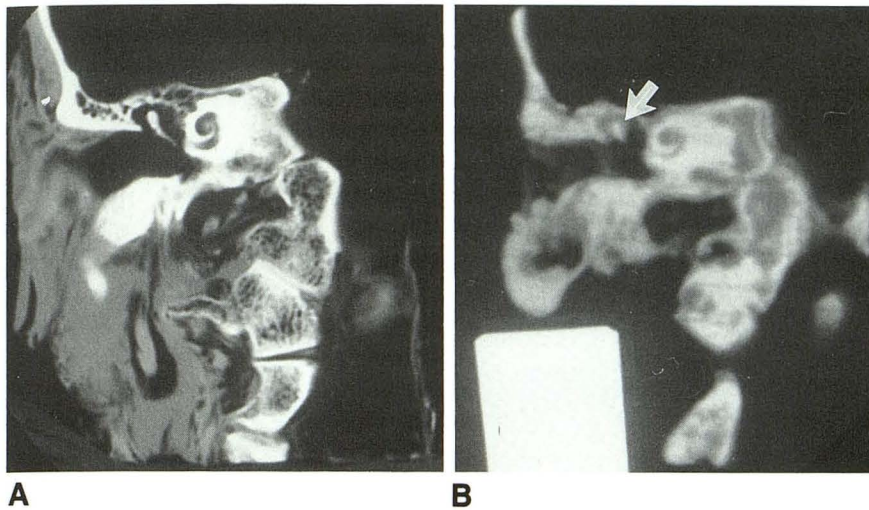
A   **B**

Fig. 2. *A,* Coronal CT image of left human cadaveric temporal bone specimen used in Figure 1. The head, neck, and manubrium of malleus are visualized. The CT image has been photographed in reverse to correspond to the orientation of the anatomic model.

B, Coronal CT image of a polycarbonate laser-sintered model generated from coronal CT data corresponding to the imaging plane in A. Only the head of the malleus is modeled (*white arrow*).

significant amount of nonsintered or partially sintered polycarbonate resulted in intermediate density on the CT images of the models.

Discussion

The utility of 3-D CT reconstructions in head and neck imaging remains controversial, having gained a number of proponents as well as those who find no significant contribution from 3-D imaging over conventional 2-D CT analysis. It may be that the ultimate usefulness of this technology lies in its ability to generate anatomic models and prostheses. Based upon prior investigations into the optimization of clinical variables that contribute to the accuracy of 3-D CT images (2, 3), a new technology, selective laser sintering, was adopted to test the relevance of these clinical variables to the model-generating process.

The term *sintering* refers to any process whereby particulates are caused to adhere into a solid mass by means of an externally applied energy. The selective laser sintering process begins with the deposition of a very thin layer of heat-fusible powder into a work-space container and heating to just below its melting point. An initial cross-section of the object under fabrication is traced on the layer of powder by a laser. In this experiment, the pattern traced by the laser is determined by a binary threshold value corresponding to a preselected Hounsfield value. Thus, the laser beam is on when the Hounsfield densities in the corresponding 2-D CT section are equal to or greater than the threshold value, and off when the Hounsfield values are less than the chosen threshold value.

The temperature of the powder impacted by the laser beam is raised to the point of sintering,

forming a solid mass. As the process is repeated, each layer fuses to the underlying layer, and successive layers of powder are deposited and sintered until the object is complete. Thus, a three-dimensional mathematical model of the surface of interest is not required for solid model generation. The laser beam intensity is modulated to sinter the powder only in areas defined by the object's design geometry. In areas not sintered, powder remains loose and serves as a natural support for the next layer of powder and the object under fabrication (4).

It is obvious that the laser beam diameter (a function of beam intensity) is greater than the individual scan line, resulting in overlap sintering of contiguous scan lines. This may be the reason fine-detail modeled structures such as the auditory ossicles appear more accurate with CT imaging than when the model is visually inspected; that is, there is a more densely sintered "core" creating greater x-ray beam attenuation than the outer, more loosely sintered coating (Fig 1).

One advantage of the selective laser sintering process is the ability to reproduce fine-detail anatomic structures within cavities (ie, the middle ear) as well as within anatomic recesses. Herein lies a major advantage over 3-D model-generating technologies, which rely upon multiaxis milling machines driven by computer-generated 3-D mathematical surface maps and which are unable to replicate enclosed cavities and are subject to tool path limitations (5).

Another advantage of selective laser sintering is the wide range of materials that comprise potential substrates. This is in contrast to an otherwise similar process, stereolithography, in which only a limited number of liquid polymers

Fig. 3. *A,* Axial CT image of left cadaveric temporal bone as in Figures 1 and 2, reversed to correspond to laser-sintered polycarbonate model in *B* and *D.* The *black arrow* indicates the head of malleus. The *black arrowhead* indicates the body of incus.

B, Laser-sintered polycarbonate model generated from axial CT data. Axial CT section through the model at the same plane as in A. The *black arrow* indicates the head of malleus. The *white arrow* indicates the body of incus.

C, Axial CT section caudal to that in A. The *white arrow* indicates the manubrium of malleus. The *black arrow* indicates the long process of incus.

D, Axial CT section through model caudal to the plane in B corresponding to C. The ossicles are not modeled.

A

B

C

D
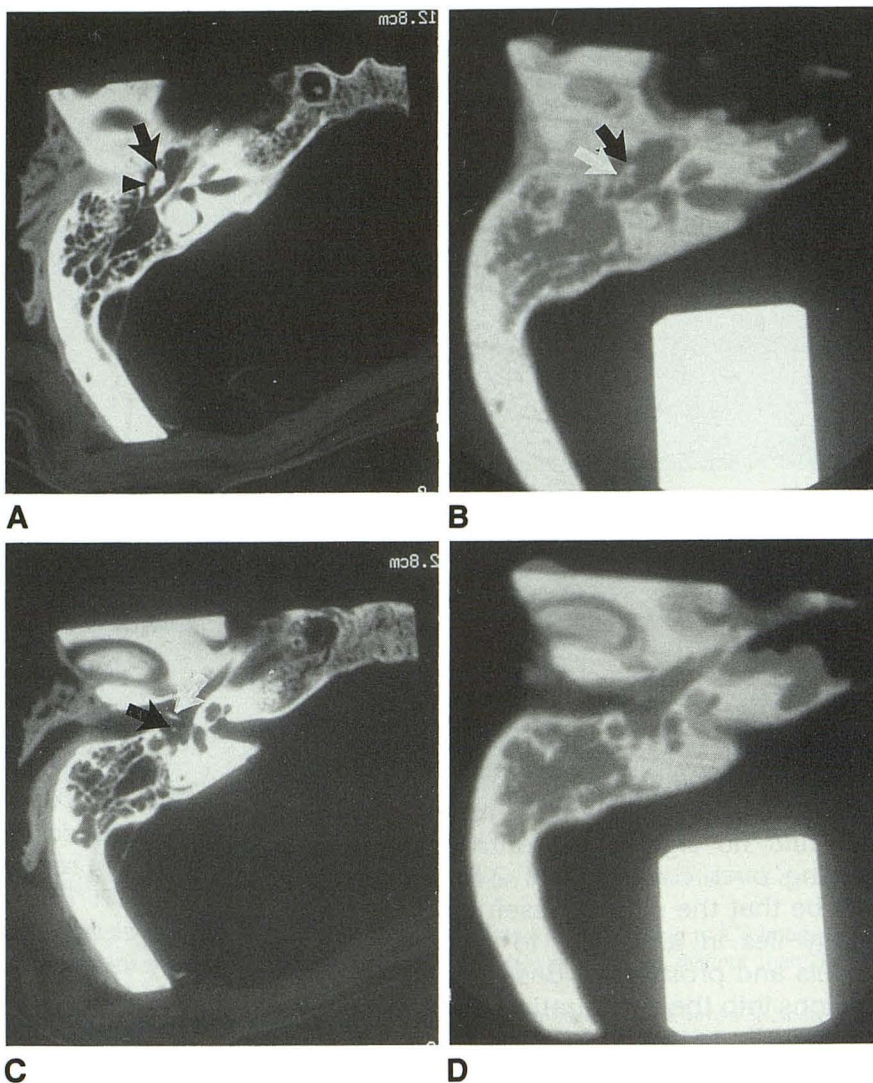
may be used (6). At present our investigations are focused on the feasibility of hydroxyapatite, a form of synthetic bone, as a substrate for the selective laser sintering process. CT/selective laser sintering–generated hydroxyapatite grafts have potential usefulness in craniofacial reconstructive surgical procedures in which experimentation with hydroxyapatite grafts is already occurring (7).

One factor in the 3-D model-generating process previously investigated in 3-D imaging is the effect of partial volume averaging via changes in CT scan plane upon the accuracy of the 3-D images (2, 3). In this research, it is assumed that with faithful transformation of 2-D CT data to toggle point format by binary thresholding, partial volume averaging in the original 2-D CT data will be manifest in the 3-D models. This may be true in this preliminary research, as evidenced by more accurate modeling of the auditory ossicles

using the sagittal CT scan plane (Fig 1). Because partial volume-averaging effects are difficult to predict (8, 9), a multiplicity of scan planes may be required to optimize the initial 2-D data set for 3-D model generation (US patent pending, serial number 07/861,947).

It must be emphasized that the potential for distortion in the models occurs not only when the layer repeat factor is improperly selected but when there is mismatch between CT pixel size and scan line dimension. In this experiment, CT pixel size was 0.25 mm and laser sintering scan line dimension 0.25 mm, and distortion in the XY plane for the axial and sagittal models did not occur. Distortion in the coronal model remains unexplained. Inaccuracy also may occur when volume-averaged pixels in the 2-D CT data are reproduced (via the layer repeat factor) through the entire section in the model. The situation is analogous to a subvoxel-sized structure in the 2-

D data set occupying an entire voxel on 3-D CT reconstruction secondary to a combination of partial volume averaging, selection of a sufficiently low binary threshold before 3-D image generation, and interpolation throughout the entire voxel volume on 3-D reconstruction.

Another artifact, analogous to aliasing in 3-D CT imaging, is the steplike borders created by successive sections in the laser sintigraphic models. Although this type of artifact can be reduced on 3-D images with the appropriate application of filtering (10), no corresponding modifications have been devised for 3-D laser sintigraphic modeling at present.

We conclude that selective laser sintering can result in accurate modeling of detailed anatomic structures in the human temporal bone. Further investigation of materials and factors contributing to the accuracy of selective laser sintering in the manufacturing of high-resolution anatomic models is justified.

Acknowledgments

References

1. Lambrecht JT, Brix F. Individual skull model fabrication for craniofacial surgery. *Cleft Palate Craniofac J* 1990;27:382–387
2. Levy RA, Edwards WT, Meyer JR, Rosenbaum AE. Facial trauma and 3-D reconstructive imaging: insufficiencies and correctives. *AJNR Am J Neuroradiol* 1992;13:885–892
3. Levy RA, Rosenbaum AE, Kellman RM, Bailey GL, Aravapalli SR. Assessing whether the plane of section on CT affects accuracy in demonstrating facial fractures in three-dimensional reconstruction using the dried skull. *AJNR Am J Neuroradiol* 1991;12:861–866
4. Nutt K. *The selective laser sintering process, new dimensions in rapid prototyping and manufacturing technologies* (monogr). DTM Corp, Austin
5. Mankovich NJ, Cheeseman AM, Stoker NG. The display of three-dimensional anatomy with stereolithographic models. *J Digit Imaging* 1990;3:200–203
6. Stoker NG, Mankovich NJ, Valentino D. Stereolithographic models for surgical planning: preliminary report. *J Oral Maxillofac Surg* 1992;50:466–471
7. Ripamonti U. Calvarial reconstruction in baboons with porous hydroxyapatite. *J Craniofac Surg* 1992;3:149–159
8. Chakeres DW. Clinical significance of partial volume averaging of the temporal bone. *AJNR Am J Neuroradiol* 1984;5:279–302
9. Goodenough D, Weaver K, Davis D, LaFalce S. Volume averaging limitations of computed tomography. *AJR Am J Roentgenol* 1982;138:313–316
10. Vannier M, Hildebolt C, Gayou D, Marsh J. Introduction to 3D imaging. In: Udupa JK, Hermann GT, eds. *3D imaging in medicine.* Boca Raton: CRC, 1991:79